Transport properties of bilayer graphene decorated by K adatoms in the framework of Thomas-Fermi screening

Sung Oh Woo,[1] Indra Yudhistira,[2] Shayan Hemmatiyan,[3] Tyler D. Morrison,[1]
K. D. D. Rathnayaka,[1] and Donald G. Naugle[1,4,*]

[1]*Department of Physics and Astronomy, Texas A&M University, College Station, Texas 77843, USA*
[2]*Department of Physics and Centre for Advanced 2D Materials, National University of Singapore, 117551, Singapore*
[3]*The James Frank Institute, The University of Chicago, Chicago, Illinois 60637, USA*
[4]*Department of Material Sciences and Engineering, Texas A&M University, College Station, Texas 77843, USA*

We report the transport properties of bilayer graphene (BLG) due to the increase of Coulomb potential fluctuations and the decrease of K adatom concentration (n_K) induced by diffusion and cluster formation of the K adatom as a function of temperature (20–300 K) and time at room temperature (RT). Upon K adatom deposition on BLG at $T = 20$ K, conductivity decreased due to the emergence of Coulomb scatterers, and the dependence of conductivity transformed from linear ($\sigma \sim n^\alpha$, $\alpha \sim 1$) to superlinear ($\alpha \sim 1.5$). As the inhomogeneity of the Coulomb potential on BLG increased by cluster formation of K adatoms, the magnitude of the conductivity increased, and the dependence of conductivity on charge carrier density (curvature) shifted towards linear behavior. We fit the experimental data with Boltzmann transport theory to show that the changes in the transport properties of BLG in the presence of charged impurities originate from two factors, n_K and the Thomas-Fermi screening vector (q_{TF}), which are both affected by cluster formation of K adatoms on BLG and the subsequent increase of Coulomb potential inhomogeneity.

I. INTRODUCTION

Since the first fabrication of graphene field effect transistor (FET) devices [1,2] single layer graphene (SLG) has attracted explosive interest and been studied extensively. As a result, fundamental properties of SLG have been determined. For example, transport properties of SLG are determined by massless Dirac fermions and a linear dispersion relation with zero gap at low energy [2], and the dominating electronic transport mechanism in SLG, charged impurity scattering, has been understood [3,4].

Bilayer graphene (BLG) consists of two graphene layers. Although BLG is a stack of two graphene layers, it reveals unique physical properties distinguished from SLG, i.e., the electronic transport properties of BLG are described by massive chiral quasiparticles with a gapless quadratic dispersion relation, $E = \pm \frac{p^2}{2m^*}$, at low energies [5,6], where $m^* = \gamma_1/2v_F^2$ is the effective mass of BLG ($v_F \sim 10^6$ m/s is the Fermi velocity of SLG and $\gamma_1 \sim 0.38$ eV is the interlayer hopping integral) [5,7,8]. Thus, the effective mass, as well as the band splitting, are attributed to the hopping integral γ_1 [9,10]. The constant 2D density of states (DOS) is also important in describing transport properties of BLG.

Due to the unique characteristics, including the energy band structure and the 2D nature of the DOS, which are distinguished from SLG, the electronic properties of BLG have been explored [11–15]. However, in contrast to SLG [3,4], the role of charged impurities in the electronic transport

of BLG has not yet been experimentally established, even though unintended charged impurities near graphene are unavoidable during processes for device fabrication. More specifically, it has been known in SLG that long- (Coulomb) and short-range scatterers contribute to the conductivity linearly ($\sigma \sim n^\alpha$, $\alpha = 1$) [3,4] and sublinearly on charge carrier density ($\sigma \sim n^\alpha$, $\alpha < 1$) [3,16], whereas the roles of these two scatterers in BLG transport have not been yet established. Theoretical studies predict that the linear dependence of conductivity ($\alpha \sim 1$) originates from the short-range scatterers, but long-range scattering mechanisms, such as the Coulomb potential, contribute to both linear ($\alpha \sim 1$) and superlinear ($1 < \alpha < 2$) conductivity behavior, depending on charge screening [7,8].

In addition, potential fluctuations in the presence of charged impurities on BLG play an important role in the transport properties of BLG through effects on Thomas-Fermi screening [7,17]. Therefore, it is important to understand the role of potential fluctuations in BLG transport in the presence of charged impurity scatterers. For controlled experiments of the transport in BLG due to charged impurity scattering, metal adatoms can be deposited on BLG. However, the charged impurity itself modifies the properties of pristine BLG, i.e., adatoms on the surface of BLG open an energy gap [11] by inducing an electric field which breaks the inversion symmetry of BLG [12–14], develop localized impurity states within the gap [18], and modify the constant DOS to a 'Mexican hat' shape in the low energy regime [14].

In spite of this modification, transport behavior of gapped BLG is not dominated by the gap or modified DOS, but by hopping through the localized states due to potential

*naugle@physics.tamu.edu

fluctuations both in Ca decorated BLG [18] and pristine BLG [13]. Moreover, transport properties of the K decorated BLG fit a theoretical model without an energy gap [19]. This indicates that there might be a dominant parameter in adatom decorated BLG other than the energy gap and the modification of the DOS due to the adatoms.

In this paper, we report transport properties of BLG decorated by K adatoms to study the role of charged impurity scattering as well as potential fluctuations in the transport properties of BLG. In order to study the effects of Coulomb potential scattering and spatial fluctuations of Coulomb potential on the transport properties of BLG, we deposited K adatoms on BLG at $T = 20$ K in ultrahigh vacuum (UHV) and subsequently increased the temperature to RT to make use of the diffusion and cluster formation behavior of K adatoms. The K adatom decorated BLG then remained in UHV at RT for four days, allowing further cluster formation of the K atoms. This process results in the decrease of both the number of isolated K adatoms, n_K, on BLG and the Thomas-Fermi screening wave vector, q_{TF}, which stems from the increase of potential fluctuations. Finally, we fit our conductivity data to Boltzmann transport theory, with emphasis on both charged impurity scattering and the Thomas-Fermi screening effect, which demonstrates that the transport properties of BLG are governed by both K adatom concentration and Coulomb screening induced by potential fluctuations.

II. EXPERIMENT

BLG FET devices were fabricated by mechanical exfoliation [2]. BLG flakes were transferred from ZYA grade highly oriented pyrolytic graphite onto SiO_2/Si substrates by sticky tape [20,21] and identified by Raman spectroscopy [22]. Heavily doped Si substrates with a thermally grown oxide layer of 285 nm thickness were used for the back gate electrode. Electrodes for contact to BLG were defined by e-beam lithography followed by thermal evaporation of chromium and gold with thicknesses of 3 nm and 50 nm, respectively. BLG FET devices were annealed at 500 K for three hours in high vacuum and degassed in UHV for one day. For atomic potassium deposition at cryogenic temperatures on BLG and subsequent *in situ* electrical transport measurements in UHV without breaking vacuum, the BLG device was mounted on the sample holder, which is connected to a liquid helium reservoir in an ultrahigh vacuum chamber [23–25]. The BLG device faces down toward the potassium metal source filament (SAES Getters) located 12" below the device. To remove impurities, the metal source filaments were preheated with an electrical current, which was gradually increased and kept at 6 A for five minutes while the UHV chamber was baked. During the deposition of K it was heated with a current of 7.5 A with a substrate temperature of 20 K. The BLG sample was surrounded by LN_2 and LHe thermal shields with shutters opened during deposition but closed at all other times. All electrical measurements were conducted with a lock-in amplifier while the BLG decorated by K adatoms remained in UHV.
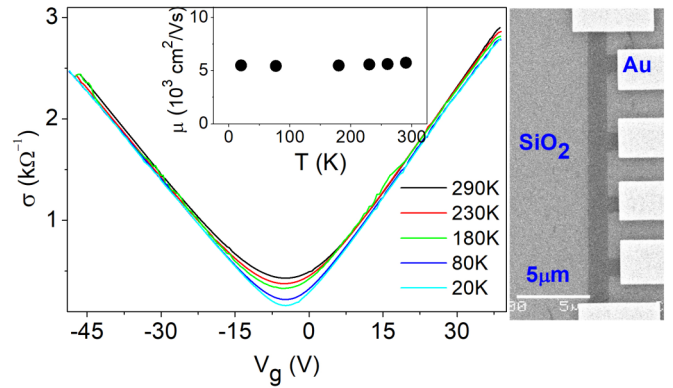
FIG. 1. Conductivity of pristine BLG as a function of gate voltage at various temperatures. The inset shows mobility calculated by $\mu = e\frac{d\sigma}{dn}$ which is extracted from the linear region of conductivity. Right panel is a SEM micrograph of a representative BLG device. The scale bar is 5 μm.

III. RESULTS AND DISCUSSION

Conductivity of pristine BLG as a function of gate voltage at various temperatures is shown in Fig. 1. Far from the charge neutrality point (V_{CNP}), the gate voltage at minimum conductivity, the conductivity in our BLG devices exhibits a weak temperature dependence and a linear dependence on charge carrier density, $\sigma(n) \sim V_g \sim n$, in good agreement with theory [8] and experiment [15]. In contrast to SLG, the transport properties of BLG have not been yet established, i.e., Zhu *et al.* [26] presented experimental results that the Hall mobility increased with both increasing temperature and charge carrier density, whereas Morozov *et al.* [15] reported experimental results that the conductivity was temperature independent and linear with charge carrier density. These differences in BLG transport may be ascribed to the detailed BLG sample conditions, such as both the concentration of defects and/or charged impurities and their spatial distribution on BLG [7,8,17]. Moreover, unintended charged impurities on the silicon substrate near BLG are unavoidable, and the transport properties of BLG are strongly influenced by charged impurities.

In order to investigate the transport behavior of BLG in the presence of Coulomb scatterers, we decorated K adatoms on BLG at $T = 20$ K with concentration of $n_K = \eta \times C_{SiO2} \times \triangle V_{CNP}/e = 3.8 \times 10^{12}$ cm^{-2}, where $\triangle V_{CNP} \sim -75$ V is the difference of V_{CNP} between pristine and K adatom decorated BLG (K/BLG), $\eta = 0.7$ is an electron transfer rate from a single K atom to BLG, $C_{SiO2} = 11.6$ nF/cm^2 is the capacitance per unit area of a 285 nm thick SiO_2 layer, and e is the elementary charge [19,25]. As shown in Fig. 2(a), the mobility of K/BLG is decreased due to the emergence of Coulomb scatterers. Another interesting transport feature of K/BLG is the transformation of the charge carrier independent mobility (black curve) to sublinear dependence (orange curve) far from V_{CNP} ($n > 1.5 \times 10^{12}$ cm^{-2}). This implies that the linear dependence of conductivity on charge carrier density in pristine BLG (Fig. 1), which can be represented by the exponent α in conductivity ($\sigma \sim n^{\alpha}$, $\alpha \sim 1$), is transformed to superlinear [black circles in Fig. 2(b)] due to K adatoms
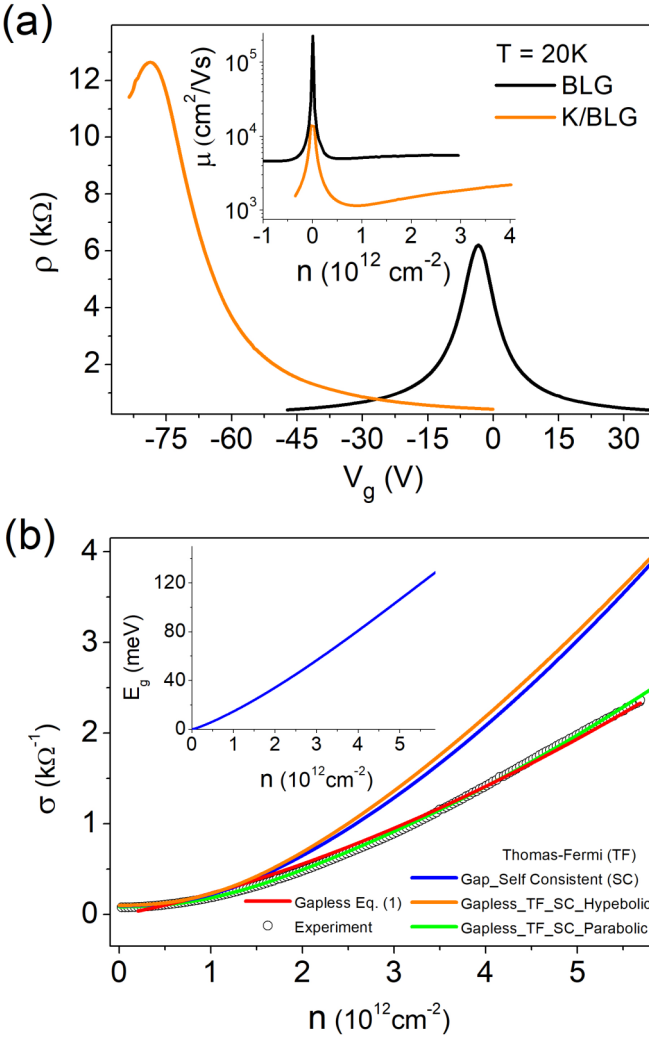
FIG. 2. (a) Resistivity of pristine and K decorated BLG at $T = 20$ K. The inset is mobility, $\mu = \sigma/ne$, of pristine (black) and K decorated BLG (orange) at $T = 20$ K. The concentration of K atoms decorated on BLG is $n_K \sim 3.8 \times 10^{12}$ cm^{-2} based on the difference of V_{CNP} before and after K adatom decoration. (b) Conductivity of the K/BLG as a function of n. Black circles are data measured at $T = 20$ K [orange curve in (a)], and the red curve is a fit with Eq. (1). Blue curve is conductivity with a gap, which is calculated based on the charge carrier density dependent energy gap [9] plotted in the inset. Orange and green curves are theoretical models, self-consistently calculated under Thomas-Fermi screening conditions with hyperbolic and parabolic energy band, respectively.

($\alpha > 1$), in agreement with the theory that α can be between 1 and 2 depending on the screening conditions [7]. To elucidate the effect of the Coulomb scatterer on the transport properties of BLG, we fit the experimental conductivity of K/BLG measured at $T = 20$ K with the Boltzmann conductivity in the presence of Coulomb scatterers, Eq. (1), which is calculated by $\sigma(n_K, q_{TF}, T) = \frac{e^2}{m} \int d\varepsilon D(\varepsilon) \cdot \varepsilon \cdot \tau(\varepsilon)(-\frac{\partial f}{\partial \varepsilon})$, where m is the effective mass of the electrons, $D(\varepsilon)$ is the density of states of BLG, f is the Fermi-Dirac distribution function, and $\tau(\varepsilon)$ is the energy dependent scattering time of electrons with K adatoms. The charge carrier scattering time is written by $\frac{\hbar}{\tau(\varepsilon_k)} = 2\pi n_K \sum_{k'} |v(q)|^2 (1 - \hat{k} \cdot \hat{k}') F(\theta) \delta(\varepsilon_k - \varepsilon_{k'})$, where $\hbar$

is the reduced Planck constant, $q = |\vec{k} - \vec{k}'| = 2k \sin\frac{\theta}{2}$ is the momentum transfer of the electron, $\hat{k} \cdot \hat{k}' = \cos\theta$, $F(\theta) = \frac{1}{2}(1 + \cos 2\theta)$, and $v(q) = \frac{2\pi e^2}{\epsilon} \frac{e^{-qd}}{q + q_{TF}}$ is the Thomas-Fermi screened Coulomb potential [7]. Under the screening condition that $2k_F < q_{TF}$ and $d \to 0$, the Boltzmann conductivity is given by

$$\sigma(n_K, q_{TF}, T)$$
$$= 0.35 q_{TF}^2 \frac{n}{n_K}\left[1 + 6.5\left(d + \frac{1}{q_{TF}}\right)\sqrt{n}\right.$$
$$+ \left\{6.5\left(d + \frac{1}{q_{TF}}\right)\right\}^2 n + \left\{4.6\left(d + \frac{1}{q_{TF}}\right)n^{-1.5}\right.$$
$$+ \left.0.79\left(d + \frac{1}{q_{TF}}\right)^2 n\right\} 10^{-7} T^2\right], \tag{1}$$

where ϵ is the dielectric constant of SiO$_2$, q_{TF} is the Thomas-Fermi screening wave vector, and d is the distance between the K atom and the top layer of BLG. As shown in Fig. 2(b), Boltzmann conductivity with zero energy gap [Eq. (1), red curve] fits well with experimental data far from V_{CNP}, in particular, the fitting parameter $n_K = 3.6 \times 10^{12}$ cm^{-2} is in good agreement with $n_K = 3.84 \times 10^{12}$ cm^{-2} calculated based on V_{CNP}, though $q_{TF} = 3.9$ nm^{-1} is higher than the theoretically predicted [7] $q_{TF} = \frac{4me^2}{\epsilon\hbar^2} \sim 1$ nm^{-1}. Here, a fixed $d = 0.3$ nm as a fitting parameter is used for the fit, but the results of fits with $d = 0.1$, 0.2, and 0.3 nm are shown further below in Fig. 4. We compare the experimental data with the self-consistent effective medium conductivity [4,27] under screening conditions [green curve in Fig. 2(b)]. Although this model fits well with the experimental data, the fitting parameter $n_K = 1.7 \times 10^{12}$ cm^{-2} is smaller than that calculated based on V_{CNP} $n_K = 3.8 \times 10^{12}$ cm^{-2}. In order to learn the contribution of an energy gap, which can appear due to the electric field generated by K adatoms on BLG [10], to K/BLG transport, we introduced a charge carrier dependent energy gap, $E_g = \frac{|U|\gamma_1}{\sqrt{U^2 + \gamma_1^2}}$, where U is the self-consistent density dependent interlayer potential given by $U = \frac{2\gamma_1 d_\perp n \sqrt{\frac{\pi}{n_0}}}{1 - 4d_\perp \sqrt{\pi n_0} \ln\left[\frac{|n|}{n_0} + \frac{1}{2}\sqrt{(\frac{n}{4n_0})^2 + (\frac{U}{2\gamma_1})^2}\right]}$ [9]. Here, $d_\perp$ is the interlayer distance between two graphene sheets, and n_0 is the density scaled corresponding to $\gamma_1/2 \equiv \hbar v_F \sqrt{n_0 \pi}$. Conductivity, taking into account a charge carrier density dependent energy gap (blue curve), significantly differs from the data with the same fitting parameters used for the gapless self consistent theory (green curve). More specifically, the conductivity taking into account the energy gap in Fig. 2(b) (blue) is greater than that of the ungapped model under screening conditions (red or green) because the Fermi energy of K/BLG is greater than the gap. In fact, the conductivity of gapped BLG (blue) is very similar to that of gapless BLG with a hyperbolic band as shown in Fig. 2(b) (orange curve), implying that the physics of the Mexican hat model is not dominated by the gap but by the density of states above the Mexican hat. This indicates that conductivity with a gapless model (red curve) under the Thomas-Fermi screening conditions describes very well the transport properties of K/BLG, and we therefore describe further transport of K/BLG with temperature and time at RT
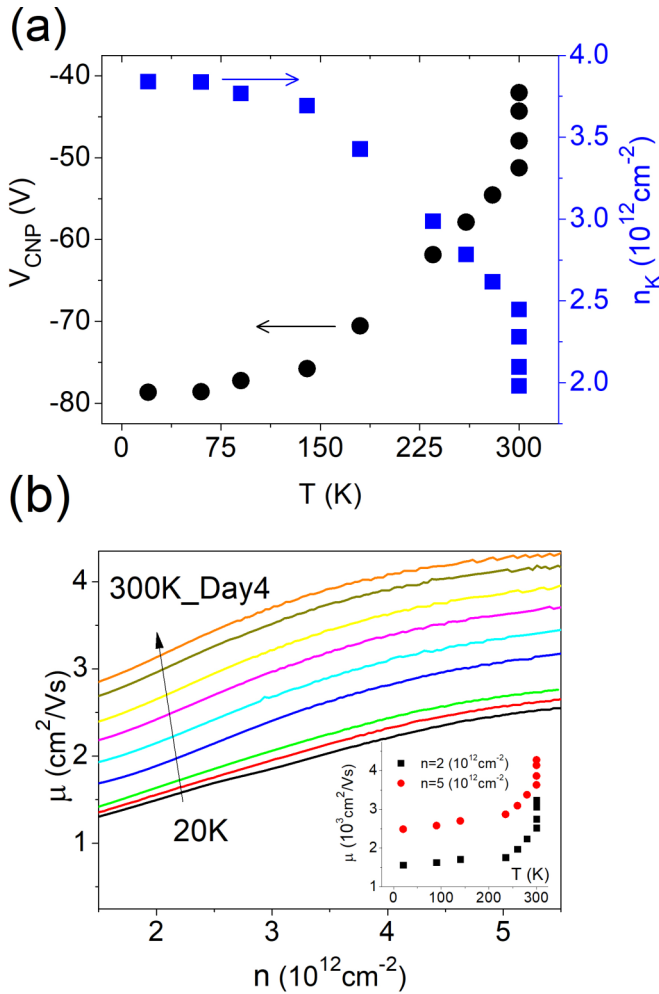
FIG. 3. Transport properties of K/BLG with temperature and time at RT. (a) V_{CNP} (black circles) and n_K (blue squares) calculated based on V_{CNP} of K/BLG with increasing temperature (20–300 K) and time at RT (four days). (b) Mobility ($\mu = \sigma/ne$) with charge carrier density higher than 1.5×10^{12} cm^{-2} is plotted at temperatures from 20 K to 300 K and with time at RT for four days). The inset is mobility extracted at $n = 2$ and 5 (10^{12} cm^{-2}).

by the Boltzmann conductivity under screening conditions, Eq. (1).

In contrast to pristine BLG, the transport properties of K/BLG strongly depend on temperature and time at RT. The V_{CNP} of K/BLG increased from -79 V to -51 V with increasing temperature from 20 K to RT and the time that K/BLG remained at RT as shown in Fig. 3(a). Recalling the experimental result by Sjövall *et al.* [28] that a submonolayer of K adatoms deposited on graphite begins to be desorbed at temperatures between 400 K and 500 K, it is reasonable to assume that potassium adatoms on BLG are not desorbed at cryogenic temperatures. Instead, cluster formation of K adatoms results in the increase of the V_{CNP} [25,29]. We observed in our previous work [25] that Li and K adatoms decorated at $T = 20$ K on SLG started to diffuse on the surface of SLG even at cryogenic temperatures, and the hopping of adatoms rapidly increased with temperature, causing cluster formation of adatoms. Therefore, it is probable that

changes in the transport properties of K/BLG originate from the dynamic behavior K adatoms. An example is that conductivity and the magnitude and the curvature of the mobility change with time at RT, as shown in Fig. 3(b). Considering the temperature independent transport properties of pristine BLG in Fig. 1, K/BLG transport probably originates from the dynamic behavior of K adatoms. Furthermore, Boltzmann theory in Eq. (1) indicates that the magnitude of conductivity, which can be converted to mobility by $\sigma = ne\mu$, is proportional to $\frac{q_{TF}^2}{n_K}$, whereas the curvature (α) is dominantly determined by $d + 1/q_{TF}$. The continuous increase in the magnitude of mobility with temperature and time (RT), as shown in Fig. 3(b), is dominated by the decrease of Coulomb scattering as evidenced by the decrease of n_K in Fig. 3(a). Regarding the curvature of transport properties of BLG, the Thomas-Fermi wave vector plays a key role in determining α as indicated by Adam *et al.* [7]. Thus, $q_{TF} = \frac{2\pi e^2}{\varepsilon} D(\varepsilon_F)$ is related to the DOS of BLG at the Fermi energy which is parameterized by Coulomb potential fluctuations [17]. Therefore, the evolution of the distribution of K adatoms with temperature and time at RT, becoming more inhomogeneous through cluster formation, increases potential fluctuations that may cause the transformation of the curvature of mobility (conductivity).

To study the relation between transport properties and Coulomb potential fluctuations on BLG, we measured conductivity with increasing temperature from 20 K to 300 K and with time at RT as shown in Fig. 4(a). We observed cluster formation of K adatoms based on the increase of V_{CNP} with temperature and time over a four day period at RT, as shown in Fig. 3(a), which increases the inhomogeneity of K on the BLG samples [29]. Given the temperature independent conductivity in pristine BLG as shown in Fig. 1 and by Morozov *et al.* [15], the increase of conductivity in Fig. 4(a) is most likely not due to thermal effects but due to the reduction of the number of isolated K adatoms on BLG by cluster formation. At RT, more importantly, the transport behavior of K/BLG continuously changes in a way that conductivity is increased, and its curvature becomes linear. Indeed, the temperature contribution in Eq. (1) to conductivity is negligibly small. Instead, the transport properties of K/BLG are affected mainly by n_K and q_{TF}. In Boltzmann transport theory within the framework of Thomas-Fermi screening, the superlinear dependence of conductivity on charge carrier density is ascribed to the factor of $d + 1/q_{TF}$ in Eq. (1). We fitted conductivity data with Eq. (1) for $d = 0.1, 0.2$, and 0.3 nm and extracted the corresponding q_{TF} and n_K, which are shown in Figs. 4(b) and 4(c), respectively. In Fig. 4(b), q_{TF} decreases with decreasing n_K for fixed d. This indicates that changes in the curvature of conductivity toward linear with increasing temperature and time at RT are due to the decrease of q_{TF}. In Fig. 4(d), to visualize the transformation of the curve, we plotted σ/n vs $n^{0.5}$. At $T = 20$ K, σ/n is linear (black curve) because the exponent α obtained by fitting conductivity with $\sigma \sim n^\alpha$ is $\sim$1.5. As the inhomogeneity of K adatoms on BLG increases with temperature and time at RT due to cluster formation, σ/n transforms from linear (black curve) to sublinear (purple curve), which is consistent with the trend of q_{TF}. As shown in Fig. 4(e), the transformation of
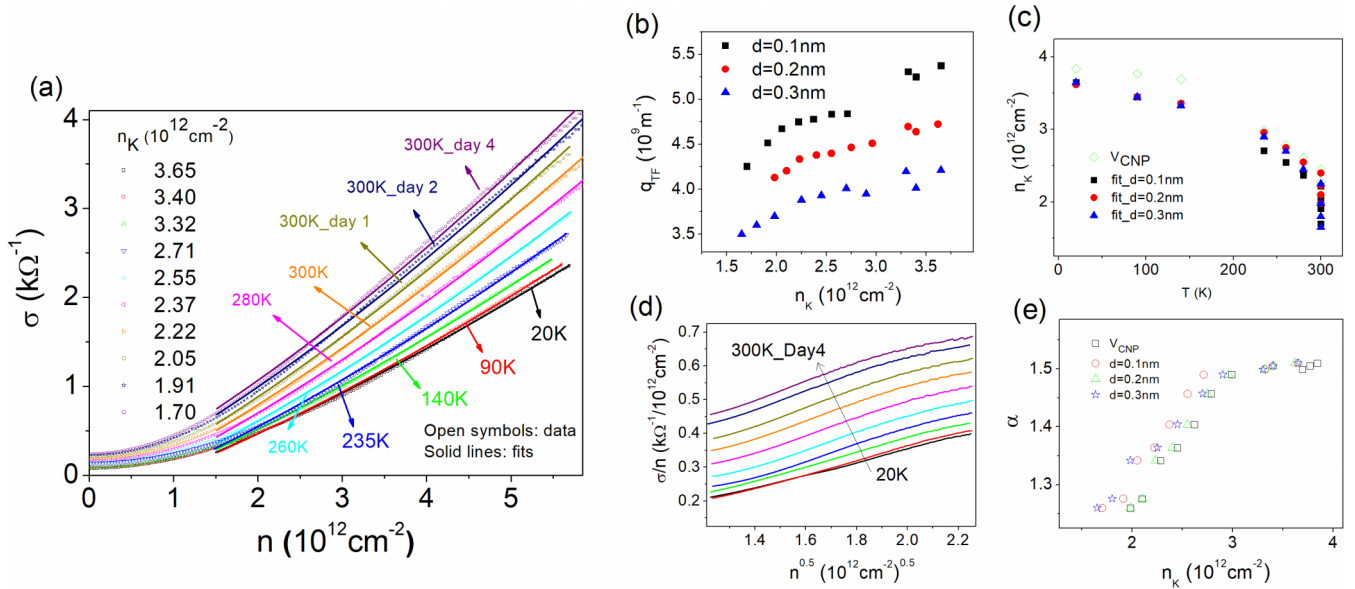
FIG. 4. Transport properties of K decorated BLG with temperature and time (at RT). (a) Conductivity as a function of charge concentration at various K adatom concentrations obtained from data fitting with Eq. (1). It shows that n_K continuously decreased with increasing temperature from 20 K to 300 K and with time at RT for four days (from bottom to top). Yellow, dark yellow, navy, and purple curves are conductivity after remaining at RT in UHV for 0, 1, 2, and 4 days, respectively. Solid lines are fits of conductivity with Eq. (1). (b) and (c) are fitting parameters n_K and q_{TF}, respectively. (d) σ/n corresponding to (a) as a function of $n^{0.5}$. (e) Plot of α, obtained by fitting conductivity with $\sigma \sim n^\alpha$, as a function of n_K calculated from V_{CNP} and the fitting parameters shown in (c).

conductivity curvature is further represented by the decrease of α from ~1.5 to ~1.2 with increasing temperature and while K/BLG remained at RT for a four-day period. In Boltzmann conductivity calculations, the simple model with a gapless quadratic energy band structure and pristine BLG DOS is used, which shows agreement with experimental data. It is obvious that an energy gap opens in BLG due to an applied electric field, in particular BLG with an electric field applied between bottom and top gates. Although an energy gap opens in K/BLG [10,18], transport properties are not dominated by the energy gap. From our data (not shown in this paper), we could not observe evidence of the energy gap opening in BLG as a result of K decoration with its concentrations ranging from 0.14 to 1.7×10^{12} cm^{-2}.

IV. CONCLUSIONS

In conclusion, we report the temperature (20–300 K) and time (300 K) dependent transport properties of BLG decorated by K adatoms at $T = 20$ K. We observed that the K adatom concentration on BLG decreases with increasing temperature from $T = 20$ K to 300 K and with time at RT, which is induced by cluster formation of K adatoms, resulting in the

increase of Coulomb potential fluctuations. Thus, the spatial fluctuation of the Coulomb potential affects the Thomas-Fermi screening condition (q_{TF}). Both changes of n_K and q_{TF} induced by the dynamic behavior of K adatoms dominate the transport properties of BLG in the presence of charged impurities.

[1] K. S. Novoselov, A. K. Geim, S. V. Morozov, D. Jiang, Y. Zhang, S. V. Dubonos, I. V. Grigorieva, and A. A. Firsov, Science **306**, 666 (2004).

[2] K. S. Novoselov, A. K. Geim, S. V. Morozov, D. Jiang, M. I. Katsnelson, S. V. Dubonos, and A. A. Firsov, Nature (London) **438**, 197 (2005).

[3] J. H. Chen, C. Jang, S. Adam, M. S. Fuhrer, E. D. Williams, and M. Ishigami, Nat. Phys. **4**, 377 (2008).

[4] S. Adam, E. H. Hwang, V. M. Galitski, and S. Das Sarma, Proc. Natl. Acad. Sci. USA **104**, 18392 (2007).

[5] E. McCann and V. I. Fal'ko, Phys. Rev. Lett. **96**, 086805 (2006).

[6] B. Partoens and F. M. Peeters, Phys. Rev. B **74**, 075404 (2006).

[7] S. Adam and S. Das Sarma, Phys. Rev. B **77**, 115436 (2008).

[8] S. Das Sarma, E. H. Hwang, and E. Rossi, Phys. Rev. B **81**, 161407(R) (2010).

[9] E. McCann and M. Koshino, Rep. Prog. Phys. **76**, 056503 (2013).

[10] T. Ohta, A. Bostwick, J. L. McChesney, T. Seyller, K. Horn, and E. Rotenberg, Phys. Rev. Lett. **98**, 206802 (2007).

[11] T. Ohta, A. Bostwick, T. Seyller, K. Horn, and E. Rotenberg, Science **313**, 951 (2006).

[12] Y. Zhang, T. T. Tang, C. Girit, Z. Hao, M. C. Martin, A. Zettl, M. F. Crommie, Y. R. Shen, and F. Wang, Nature (London) **459**, 820 (2009).

[13] K. Zou and J. Zhu, Phys. Rev. B **82**, 081407(R) (2010).

[14] E. V. Castro, K. S. Novoselov, S. V. Morozov, N. M. R. Peres, J. M. B. Lopes dos Santos, J. Nilsson, F. Guinea, A. K. Geim, and A. H. Castro Neto, Phys. Rev. Lett. **99**, 216802 (2007).

[15] S. V. Morozov, K. S. Novoselov, M. I. Katsnelson, F. Schedin, D. C. Elias, J. A. Jaszczak, and A. K. Geim, Phys. Rev. Lett. **100**, 016602 (2008).

[16] K. Nomura and A. H. MacDonald, Phys. Rev. Lett. **98**, 076602 (2007).

[17] Q. Z. Li, E. H. Hwang, and S. Das Sarma, Phys. Rev. B **84**, 115442 (2011).

[18] Q. Han, B. Yan, Z. Jia, D. Yu, and X. Wu, Appl. Phys. Lett. **107**, 163104 (2015).

[19] S. D. Xiao, J. H. Chen, S. Adam, E. D. Williams, and M. S. Fuhrer, Phys. Rev. B **82**, 041406(R) (2010).

[20] S. Woo and W. Teizer, Appl. Phys. Lett. **103**, 041603 (2013).

[21] S. Woo and W. Teizer, Carbon **93**, 693 (2015).

[22] A. C. Ferrari, J. C. Meyer, V. Scardaci, C. Casiraghi, M. Lazzeri, F. Mauri, S. Piscanec, D. Jiang, K. S. Novoselov, S. Roth, and A. K. Geim, Phys. Rev. Lett. **97**, 187401 (2006).

[23] D. G. Naugle, B. Bandyopadhyay, Y. Bo, V. M. Nicoli, F. C. Wang, and K. D. D. Rathnayaka, Rev. Sci. Instrum. **58**, 1271 (1987).

[24] P. W. Watson and D. G. Naugle, Phys. Rev. B **51**, 685 (1995).

[25] S. Woo, S. Hemmatiyan, T. D. Morrison, K. D. D. Rathnayaka, I. F. Lyuksyutov, and D. G. Naugle, Appl. Phys. Lett. **111**, 263502 (2017).

[26] W. Zhu, V. Perebeinos, M. Freitag, and P. Avouris, Phys. Rev. B **80**, 235402 (2009).

[27] E. Rossi, S. Adam, and S. Das Sarma, Phys. Rev. B **79**, 245423 (2009).

[28] P. Sjövall, Surf. Sci. **345**, L39 (1996).

[29] Y. Wang, S. Xiao, X. Cai, W. Bao, J. Reutt-Robey, and M. S. Fuhrer, Sci. Rep. **5**, 15764 (2015).